arXiv:1302.1429v1 [cond-mat.supr-con] 6 Feb 2013

Weak-coupling superconductivity in $NaFe_{0.975}Co_{0.025}As$ from NMR Knight shift and penetration depth

Sangwon Oh[1], A. M. Mounce[1], J. S. Lee[1], W. P. Halperin[1], C. L. Zhang[2], S. Carr[2], Pengcheng Dai[2]
[1] *Department of Physics and Astronomy, Northwestern University, Evanston, Illinois 60208, USA*
[2] *Department of Physics and Astronomy, The University of Tennessee, Knoxville, Tennessee 37996, USA*
(Dated: Version February 7, 2013)

Based on ARPES and STM work, Co doped NaFeAs has been reported to be a strongly coupled superconductor, similar to cuprates [1–3]. However, a recent ARPES result, claims otherwise, with $2\Delta/k_BT_c$ slightly beyond the BCS limit, 3.53 [4]. We have performed ^{75}As and ^{11}Na nuclear magnetic resonance(NMR) on high-quality, single crystals of $NaFe_{0.975}Co_{0.025}As$. The temperature dependence of the ^{75}As Knight shift, fitted to a Yosida function, suggests moderately weak-coupling superconductivity in a singlet state with $2\Delta/k_BT_c = 4.0 \pm 0.3$. The temperature dependence of the penetration depth obtained from ^{11}Na NMR was found to be consistent with the Knight shift results and $\lambda_{ab}(0)$ was found to be $5,327 \pm 78\mathring{A}$.

PACS numbers:

Superconductors have been classified as weak or strong coupling depending on the amplitude of the energy gap relative to T_c where $2\Delta/k_BT_c = 3.53$ is the weakcoupling BCS limit. Larger values can be associated with strong coupling and a possible indication of strong electronic correlations. ^{3}He, cuprate superconductors, and heavy fermion materials are in this class. However, a consistent picture for the recently discovered pnictide superconductors has not yet emerged with a wide spread in the reports of $2\Delta/k_BT_c$ [5] from 1 to 8. K-subsitituted $BaFe_2As_2$ (hole doped) has doping independent behavior, $2\Delta/k_BT_c \sim 3.1$, found from point contact Adreev reflection (PCAR), whereas Co-substituted $BaFe_2As_2$ (electron doped) shows doping dependence with strong coupling superconductivity near optimal doping [6, 7]. It might be inferred, therefore, that Co-substituted NaFeAs (electron doped) should also be strongly coupled, and indeed this was reported from angle resolved photoemission spectroscopy (ARPES) and scanning tunneling microscopy (STM) [1–3, 8]. However, recent ARPES experiments question these claims arguing that the superconducting gap size had been over-estimated owing to larger impurity scattering rates [4]. Since ARPES and STM measurements are surface sensitive, it is important to investigate these issues with a probe that detects bulk superconductivity. NMR satisfies these requirements, and here we report that superconductivity in $NaFe_{0.975}Co_{0.025}As$ (NaCo25) has moderately weak-coupling from the temperature dependence of the Knight shift and penetration depth in high-quality NaCo25, taken from measurements of ^{75}As and ^{11}Na NMR respectively.

Our ^{75}As and ^{11}Na NMR experiments were performed at Northwestern University from 4.2 K to room temperature with external magnetic field $H = 6.4$ T parallel to the c-axis. Because of the high reactivity of Na we used an environmentally sealed sample holder, Fig. 1 (a), made out of glass, for ^{75}As NMR, or Stycast 1266® for ^{11}Na. The containers were filled with He in an oxygen free chamber to prevent sample degradation and to exchange heat. Degradation can be identified over time from an increase in the NMR linewidth and consequently different crystals were used for ^{75}As and ^{11}Na NMR. In the work we report here, both exhibited very narrow NMR spectra at room temperature: 8 kHz for ^{75}As, and 3 kHz for ^{11}Na. Crystals with dimensions $\sim 3\times2\times0.3\,\mathrm{mm}^3$ were grown at the University of Tennessee and found to have T_c of 21 K from magnetization with $H = 10$ G parallel to the ab-plane, Fig. 1 (b). Typically, spin-echo sequences ($\pi/2$ - π) were used to obtain spectra, Knight shift, and spin-lattice relaxation rate, $1/T_1$, for the central transition (-1/2 $\leftrightarrow$1/2) with a π-pulse $\approx$ 8 μsec. The spin-spin relaxation time, T_2, was measured with a Carr-Purcell-Meiboom-Gill (CPMG) sequence and T_1 was measured with the usual saturation recovery method when it was shorter than 2 sec. For longer T_1 the more efficient progressive saturation technique [9] was used.

The ^{75}As and ^{11}Na NMR spectra from the central transitions are shown in Fig. 1 (c) and (d). The narrow linewidths of the spectra in the normal state, 10 kHz (^{75}As) and 3 kHz (^{11}Na) at 20 K, and their very weak dependence on temperature are indications of high crystal quality. In the normal state, cooling from high temperatures, both ^{75}As and ^{11}Na spectra shift to lower frequency as has been observed in other pnictide superconductors [10–12]. Below $T_c = 18$ K in 6.4 T, the abrupt decrease in the ^{75}As spectra indicates a spin-singlet transition. Formation of the vortex lattice is evident in broadening of the spectra in the superconducting state.

The measured NMR frequency shift, $\Delta\omega(T)$, relative to the Larmor frequency, $\Delta\omega(T)/\omega_L = (\omega(T) - \omega_L)/\omega_L$, can be expressed as,

$$K(T) = K_s(T) + K_{orb} + K_Q + 4\pi(1 - D)M(T)/H, \quad (1)$$

generically referred to as the Knight shift, ^{75}K and ^{11}K for each nucleus, determined from the peak posi-

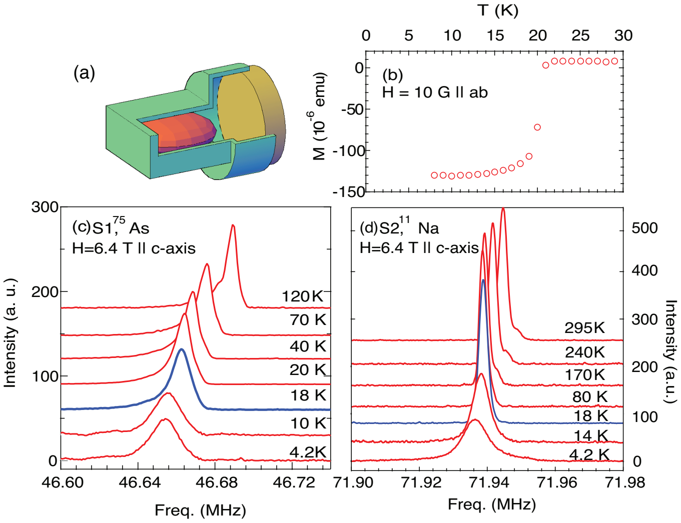

FIG. 1. (a) Schematic drawing of the sample holder; (b) magnetization measurements; (c, d) NMR spectra of NaCo25 in 6.4 T with H || c-axis. The narrow linewidths confirm high sample quality. As with other pnictide superconductors [10–12] NaCo25 shows a continuous decrease on cooling from room temperature above T_c. Below $T_c = 18$ K (blue trace) the spectra shift noticeably to lower frequency with decreasing temperature indicating spin-singlet superconductivity in NaCo25. The increased linewidth on cooling below T_c is due to the formation of a vortex lattice.

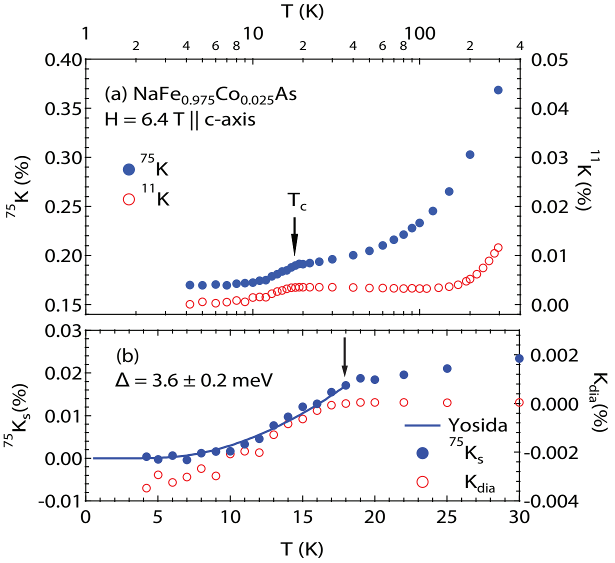

FIG. 2. Knight shifts for ^{75}As and ^{11}Na over a wide temperature range. (a) The decrease of K in the normal state on cooling is characteristic of pnictide superconductors. (b) The low temperature behavior of $^{75}K_s$, after subtraction of K_{dia}, is fitted to a Yosida function[13], solid curve, with $2\Delta(0)/k_BT_c = 4.0$ which we interpret as evidence for moderately weak-coupling superconductivity.

tions of the spectra in Fig. 2. The Knight shift has electron spin, K_s, orbital, K_{orb}, quadrupolar, K_Q, and K_{dia} terms, the latter from the superconducting diamagnetism, $M(T)$ with demagnetization factor, D; K_{orb} and K_Q provide a temperature independent offset. In the normal state the temperature dependence comes from $K_s(T) = \chi_s(T)A_{hf}$, given by the spin susceptibility, $\chi_s(T)$, and its corresponding hyperfine coupling, A_{hf}. For $T > 100$ K the different temperature dependence of ^{75}K and ^{11}K is due to a much smaller hyperfine field for Na as compared to As, which we estimate to be $^{75}A_{hf}/^{11}A_{hf} \approx 19$. For $T < 100$ K the comparison of ^{11}K with ^{75}K indicates $^{11}K_s$ is negligible and $^{11}K_{orb} +^{11} K_Q = 0.0033\,\%$. The decrease of ^{11}K in the superconducting state is due entirely to $K_{dia}(T)$ and provides an internal measure of the local field that can be subtracted from ^{75}K to give a precise determination of the spin shift, $^{75}K_s(T < T_c)$, Fig. 2(b).

We assume a single isotropic superconducting energy gap in NaCo25. Even though the sizes of the superconducting gaps from different ARPES measurements in NaFe$_{0.95}$Co$_{0.05}$As (NaCo50) are different, they are consistent in two ways: no anisotropy in the superconducting gaps in NaCo50, and the sizes of the superconducting gaps on the electron and hole Fermi surfaces are almost identical [1, 4]. Consequently, we fit the temperature dependence of $^{75}K_s$ to an isotropic Yosida function, $Y(T)$ [13], Eq. 2, to determine $\Delta(T)$. We take the gap to be scaled [14] to the weak-coupling BCS superconducting gap, $\Delta_0(T)$, represented in Eq. 3 by a convenient analytical form [15], and then we fit the measured Knight shift to determine the scale factor α and hence $\Delta(0)$.

For $T < T_c$,

$$\frac{K_s(T)}{K_s(T_c)} = Y(T) = 1 - 2\pi k_B T \sum_{n=0}^{\infty} \frac{\Delta(T)^2}{(\epsilon_n^2 + \Delta(T)^2)^{3/2}} \tag{2}$$

$$\Delta(T) = \alpha\Delta_0(T) \tag{3}$$

$$\Delta_0(T) = \Delta_0(0)\tanh\left(\frac{k_BT_c\pi}{\Delta_0(0)}\sqrt{\frac{2}{3}\left(\frac{T_c}{T} - 1\right)\left.\frac{\Delta C}{C}\right|_0}\right) \tag{4}$$

where $\epsilon_n = 2\pi(n + 1/2)k_BT$ [16] and $\frac{\Delta C}{C}|_0$ is 1.43. With this procedure we have found the superconducting gap size to be 3.6 ± 0.3 meV, $2\Delta/k_BT_c = 4.0$, and $\alpha = 1.14 \pm 0.1$. The resultant fit is shown in Fig. 2.(b). Our result is slightly larger than the BCS limit but still supports the basic idea that superconductivity in NaCo25 is weakly-coupled consistent with a recent ARPES measurements [4]. The Knight shift is a thermodynamic measurement and at low temperatures is sensitive to the low lying excitations $\lesssim 1$ meV above the energy gap. If indeed there are two gaps of comparable size we should interpret our results in terms of the smaller of these. Recent STM measurements [8] on the same material, and from the same source as ours, infer a larger energy gap of 5.5 meV. It is interesting that the bosonic mode reported in that work is within 8% in energy to 2Δ inferred from the Knight shift. The disparity in energy gap size between Knight shift and STM may be a reflection of the different sensitivity in the two experiments to gap structure and energy scales.

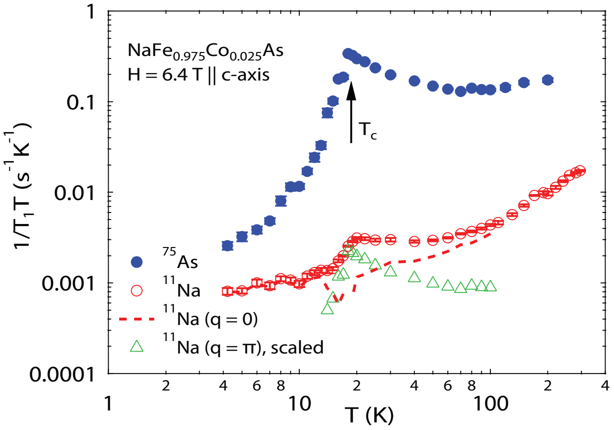

FIG. 3. The spin-lattice relaxation rate divided by temperature, $1/T_1T$, from ^{75}As and ^{11}Na. The increase of $1/^{75}T_1T$ (blue circles) on cooling in the normal state is due to spin fluctuations [12], and drops for $T < T_c$ with the onset of superconductivity. Despite the small hyperfine field, $1/^{11}T_1T$, has a similar behavior near T_c (red circles). Scaling the rates by the square of the ratio of the hyperfine fields and their respective gyromagnetic ratios gives the open green triangles for the expected contribution at the Na site. What remains is a second component of relaxation (red dashed curve) of unknown origin.

In contrast to the Knight shift ($\omega \approx 0, q \approx 0$) the spin-lattice relaxation is determined by the sum over wave vectors, q, of the imaginary part of the dynamic susceptibility which is coupled to the nucleus through the square of the hyperfine field given by the form factor, $F(q)$, Eq. 5,

$$1/T_1T \propto \gamma^2 \sum_q F(q) \frac{Im[\chi_\perp(q,\omega)]}{\hbar\omega} \tag{5}$$

where γ is the gyromagnetic ratio, $F(q)$ the form factor, Im $[\chi_\perp]$ is the imaginary part of the dynamic susceptibility perpendicular to the field.

We have found different behavior for $1/^{75}T_1T$ and $1/^{11}T_1T$, Fig. 3. In the normal state, $1/^{75}T_1T$ increases with decreasing temperature approaching T_c and can be understood in terms of spin fluctuations [11, 12, 17, 18] expressed in terms of the Moriya theory [19], Eq.5. The increase is suppressed with the onset of superconductivity, so that $1/^{75}T_1T$ drops dramatically below T_c, apparently strongly dependent on the density of normal quasiparticle excitations. For Na we find that $1/^{11}T_1T$ has a component that mimics this behavior and can be accounted for by the weak hyperfine coupling strength, $^{11}A_{hf}$. Scaling the rates by the square of the ratio of the hyperfine fields and their respective gyromagnetic ratios, gives the open green triangles in Fig. 3. Subtracting this spin-fluctuation component of $1/^{11}T_1T$ leaves a second contribution represented by the dashed red curve. We speculate that the spin-fluctuations come from $q \approx \pi$ and that the remainder might be from, $q \approx 0$, not significantly affected by superconductivity.

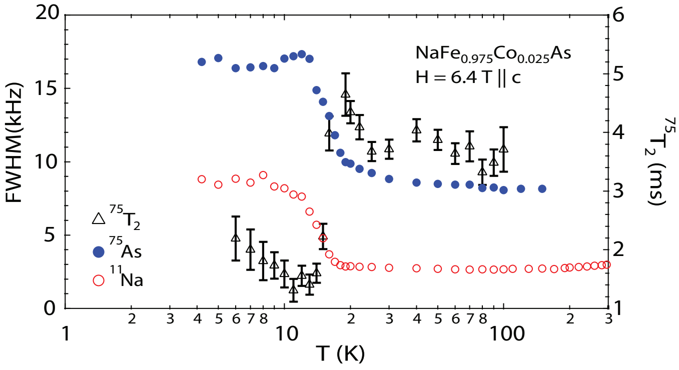

FIG. 4. Temperature dependence of the linewidth, full-width at half-maximum (FWHM), of the ^{75}As and ^{11}Na central transition, and the spin-spin relaxation time, T_2. The narrow linewidths at $T = 20$ K from ^{75}As (10 kHz) and ^{11}Na (3 kHz) and the weak temperature dependences indicate high crystal quality. Below T_c the linewidth increases in the inhomogeneous vortex state and becomes constant below ≈ 13 K for ^{75}As (12 K for ^{11}Na).

We next turn our discussion to the diamagnetism and vortex supercurrents in the superconducting state. The linewidths of the central transitions of ^{75}As and ^{11}Na are shown in Fig. 4. Below T_c the linewidths from both samples broaden due to vortices and approach a constant at low temperature approximately at the minimum in $^{75}T_2$, which we identify with the formation of a robust vortex solid. In our earlier work on Co doped BaFe$_2$As$_2$ [10] we have associated a minimum T_2 with the irreversibility temperature where vortices become pinned. Although ^{11}Na NMR is not as effective as ^{75}As NMR for probing the electronic excitations, it nonetheless provides a higher resolution tool for analysis of the spectrum in the superconducting state which is affected by vortices and from which we can determine the penetration depth, λ_{ab}. The comparisons between the superconducting state spectra and the normal state spectra in Fig. 5, indicate an increase in the high frequency portion of the spectrum as expected in a vortex solid. We have solved the Ginzburg-Landau (GL) equations in an ideal vortex lattice using Brandt's algorithm [21], where we set $H_{c2} = 36$ T [22]. The resulting best fit distribution of local fields for ^{11}Na at $T = 4.2$ K is presented in Fig. 5 (c). The fit was performed by convoluting the GL solution from the algorithm and the normal state ($T = 20$ K) spectrum, minimizing its difference from the experimental spectra using the penetration depth as an adjustable parameter. We have an-

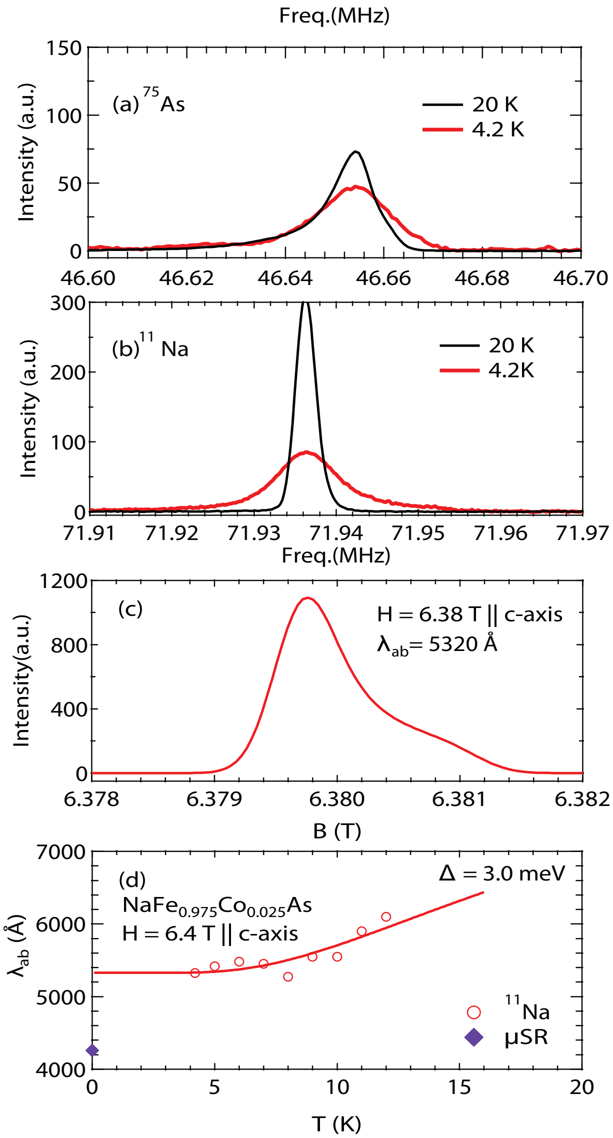

FIG. 5. Spectra in the normal state (20 K, shifted in frequency for comparison) and the superconducting state (4.2 K) for (a)^{75}As and (b)^{11}Na. The linewidth broadening due to vortices is evident in the superconducting state, especially clear for ^{11}Na. (c) The Ginzburg-Landau calculation that best fits the superconducting state ^{11}Na spectra at $T = 0$ K from which the penetration depth, λ_{ab}, was determined. (d) Penetration depth as a function of temperature where $\lambda_{ab}(0)$ is $5,327 \pm 78\,\mathring{A}$. Temperature dependence of the penetration depth is shown in (d) compared with a μSR experiment, $\lambda_{ab}(0) = 4,260\,\mathring{A}$ [20]. Fitting to a BCS formula we found the superconducting gap to be 3.0 ± 0.3 meV consistent with Knight shift data.

alyzed $\lambda_{ab}(T)$ using a BCS formula in the low temperature limit, $\lambda(T) = \lambda(0)[1 + \sqrt{\frac{\pi\Delta}{2k_BT}}\exp(-\frac{\Delta}{k_BT})]$ [23]. For ^{75}As we find $\lambda_{ab}(0)$ to be $4,780\,\mathring{A}$ and from ^{11}Na, $\lambda_{ab}(0) = 5,327\,\mathring{A}$, which can be compared with μSR [20], $\lambda_{ab}(0) = 4,260\,\mathring{A}$. The penetration depth from the ^{11}Na is more reliable since the temperature dependent spin shift is negligible. From the BCS fit we found the superconducting gap size 3.0 ± 0.4 meV, close to the value from the Knight shift, supporting the view that NaCo25 superconductivity is close to weak-coupling.

In summary, we have found evidence for moderately weak-coupling superconductivity from the Knight shift and the penetration depth in NaCo25. The superconducting gap sizes, 3.6 ± 0.3 meV, from the Knight shift and 3.0 ± 0.4 meV from the penetration depth are consistent with $2\Delta/k_BT_c = 4.0 \pm 0.3$ taken from the Knight shift results. Additionally, the spectra in the mixed state have been successfully represented in Ginzburg-Landau theory, giving a penetration depth of $\lambda_{ab}(0) = 5,327 \pm 78\,\mathring{A}$.

ACKNOWLEDGMENTS

Research was supported by the U.S. Department of Energy, Office of Basic Energy Sciences, Division of Materials Sciences and Engineering under Awards DE-FG02-05ER46248 (Northwestern University). The single crystal growth at the University of Tennessee was supported by U.S. DOE, BES under grant No, DE-FG02-05ER46202(P.D.)

[1] Z. H. Liu *et al.*, Phys. Rev. B. **84**, 064519 (2011).
[2] P. Cai *et al.*, (2012), arXiv.org:1208.3842v1..
[3] H. Yang *et al.*, Phys. Rev. B. **86**, 214512 (2012).
[4] S. Thirupathaiah *et al.*, Phys. Rev. B **86**, 214508 (2012).
[5] D. S. Inosov *et al.*, Phys. Rev. B **83**, 214520 (2011).
[6] X. Zhang *et al.*, Phys. Rev. B **82**, 020515 (2010).
[7] F. Hardy *et al.*, EPL. **91**, 47008 (2010).
[8] Z. Wang *et al.*, Nature Physics **9**, 42 (2013).
[9] V. F. Mitrović, E. E. Sigmund, and W. P. Halperin, Phys. Rev. B. **64**, 024520 (2001).
[10] S. Oh *et al.*, Phys. Rev. B **83**, 214501 (2011).
[11] S. Oh *et al.*, Phys. Rev. B **85**, 174508 (2012).
[12] F. L. Ning *et al.*, Phys. Rev. Lett. **104**, 037001 (2010).
[13] K. Yosida, Phys. Rev. **110**, 769 (1958).
[14] H. Padamsee, J. E. Neighbor, and C. A. Shiffman, J. Low Temp. Phys. **12**, 387 (1973).
[15] W. P. Halperin and E. Varoquaux, in *Helium Three*, Modern Problems in Condensed Matter Sciences, Vol. 26, edited by W. P. Halperin and L. P. Pitaevskii (Elsevier, 1990) Chap. 7, p. 353.
[16] J. A. Sauls, Private communication.
[17] K. Kitagawa *et al.*, J. Phys. Soc. Jpn. **80**, 033705 (2011).
[18] Z. Li *et al.*, Phys. Rev. B **83**, 140506 (2011).
[19] T. Moriya, J. Phys. Soc. Jpn. **18**, 516 (1963).
[20] D. Parker *et al.*, Phys. Rev. Lett. **104**, 057007 (2010).
[21] E. H. Brandt, Phys. Rev. Lett. **78**, 2208 (1997).
[22] S. Y. Zhou *et al.*, (2012), arXiv.org:1204.3440v2..
[23] R. Prozorov and W. Giannetta, Supercond. Sci. Technol. **19**, 41 (2006).